

3. Xue, Y., Wu, S., Hou, H. and Zha, J., Experimental investigation of basic oxygen furnace slag used as aggregate in asphalt mixture. *J. Hazard. Mater.*, 2006, **138**, 261–268.
4. Wu, S., Xue, Y., Ye, Q. and Chen, Y., Utilization of steel slag as aggregates for stone mastic asphalt (SMA) mixtures. *Build. Environ.*, 2007, **42**, 2580–2585.
5. Shen, D. H., Wu, C. M. and Du, J. C., Laboratory investigation of basic oxygen furnace slag for substitution of aggregate in porous asphalt mixture. *Constr. Build. Mater.*, 2009, **23**, 453–461.
6. Motz, H., In Proceedings of the 3rd European Slag Conference, Brussels, Belgium, 2003, pp. 120–123.
7. Mack, B. and Gutta, B., An analysis of steel slag and its use in acid mine drainage (AMD) treatment. In National Meeting of the American Society of Mining and Reclamation, Billings, MT, Revitalizing the Environment: Proven Solutions and Innovative Approaches (ed. Barnhisel, R. I.), ASMR, 3134 Motavesta Rd., Lexington, KY 40502, 30 May–5 June 2009.
8. Pinto, C. G. and Gomes, J. F. P., Leaching of heavy metals from steelmaking slags. *Rev. Metall. (Paris)*, 2006, **42**, 409–416.
9. Gahan, C., Cunha, M. and Sandstrom, A., Comparative study on different steel slags as neutralizing agent in bioleaching. *Hydrometallurgy*, 2009, **95**, 190–197.
10. Ziemkiewicz, P., Steel slag: applications for AMD control. In Proceedings of the Conference on Hazardous Waste Research, Morgantown, WV 26505-6064, 1998, pp. 44–62.
11. Langova, S. and Matysek, D., Zinc recovery from steel-making wastes by acid pressure leaching and hematite precipitation. *Hydrometallurgy*, 2010, **101**, 171–173.
12. Proctor, D., Physical and chemical characteristics of blast furnace, basic oxygen furnace, and electric arc furnace steel industry slags. *Environ. Sci. Technol.*, 2000, **34**, 1576–1582.
13. Pinto, M., Rodriguez, M., Besga, M., Balcazar, N. and Lopez, F. A., Effects of Linz-Donowitz (LD) slag on soil properties and pasture production in the Basque Country (Northern Spain). *N.Z. J. Agric. Res.*, 1995, **38**, 143–155.
14. Marr, I. L., Kluge, P., Main, L., Margerin, V. and Lescop, C., Digests or extracts? – Some interesting but conflicting results for three widely differing polluted sediment samples. *Mikrochim. Acta*, 1995, **119**, 219.
15. Krause, P., ErbsloÈh, B., NiedergesaÈù, R., Pepelnik, R. and Prange, A., Comparative study of different digestion procedures using supplementary analytical methods for multielement-screening of more than 50 elements in sediments of the river Elbe. *Fresenius. J. Anal. Chem.*, 1995, **353**, 3.
16. Tsolakidou, A., Garrigós, J. B. I. and Kilikoglou, V., Assessment of dissolution techniques for the analysis of ceramic samples by plasma spectrometry. *Anal. Chim. Acta*, 2002, **474**, 177–188.
17. US Environmental Protection Agency, Test Methods for Evaluating Solid Waste: Physical/Chemical Methods, EPA SW-846, US Government Printing Office, Washington DC, 1986, 3rd edn.

**ACKNOWLEDGEMENTS.** We thank Dr Sanjay Chandra, Tata Steel Limited, Jamshedpur for providing an opportunity to work on this project. We also thank the staff of Chemical Lab Division, Tata Steel Limited, Jamshedpur for support.

Received 9 October 2017; revised accepted 29 May 2018

doi: 10.18520/cs/v115/i5/973-977

## Preparation of nanosized bioapatite by cryogenic grinding from sintered scales of silver carp *Hypophthalmichthys molitrix* (Cuvier and Valenciennes)

Ravneet<sup>1,\*</sup>, Gaurav Verma<sup>2,3</sup>, Bandu Matiyal<sup>1</sup> and Neha Thakur<sup>1</sup>

<sup>1</sup>Department of Zoology, Panjab University, Chandigarh 160 014, India

<sup>2</sup>Dr S. S. Bhatnagar University Institute of Chemical Engineering and Technology, Panjab University, Chandigarh 160 014, India

<sup>3</sup>Centre for Nanoscience and Nanotechnology (UIEAST), Panjab University, Chandigarh 160 014, India

The present study is based on the processing of bio-apatite (BAp) of sintered fish scales, i.e. heat treated fish scales at 900°C, by the cryogenic grinding technique. It shows that BAp formed by cryogenic grinding of sintered fish scales became purer and nanosized. Earlier studies had reported that nanosized bioapatite increases the resorbability and bioactivity for tissue replacement and regeneration like bones and dental tissues of human beings. Energy dispersive X-ray spectroscopy of sintered fish scale BAp confirmed the presence of tetracalcium phosphate with Ca/P ratio of 1.97. Field emission scanning electron microscopy and dynamic light scattering (DLS) showed microsized particles. The sintered fish scales when cryoground showed the formation of nanosized particles as revealed by transmission electron microscopy and DLS. The Fourier transform infrared spectroscopy results of sintered and cryoground BAp had similar functional groups, but cryoground BAp showed greater purity.

**Keywords:** Bioapatite, biogenic source, cryogenic grinding, fish scales, sintering.

RECENT years have witnessed exponential research growth in the area of nanoscience and nanotechnology and their bio-applications. Nanoparticles have the ability to partially dissolve during fibre attachment; so they can be used as a novel implant component. It is believed that nanosized bioapatite (BAp), isolated or prepared from biogenic sources, is most appropriate for tissue replacement and regeneration. It exhibits enhanced resorbability and much higher bioactivity than micron-sized or synthetic hydroxyapatite (HAp)<sup>1</sup>.

Fish biowaste, such as scales which are dumped as waste due to their unexplored commercial value, contains several types of calcium salts<sup>2</sup>. These fish scales can be used to isolate hydroxyapatite or bioapatite to be exploited in the research and development of useful biomaterials in the field of bone implantation, fabrication and fixation.

\*For correspondence. (e-mail: ravneet16@pu.ac.in)

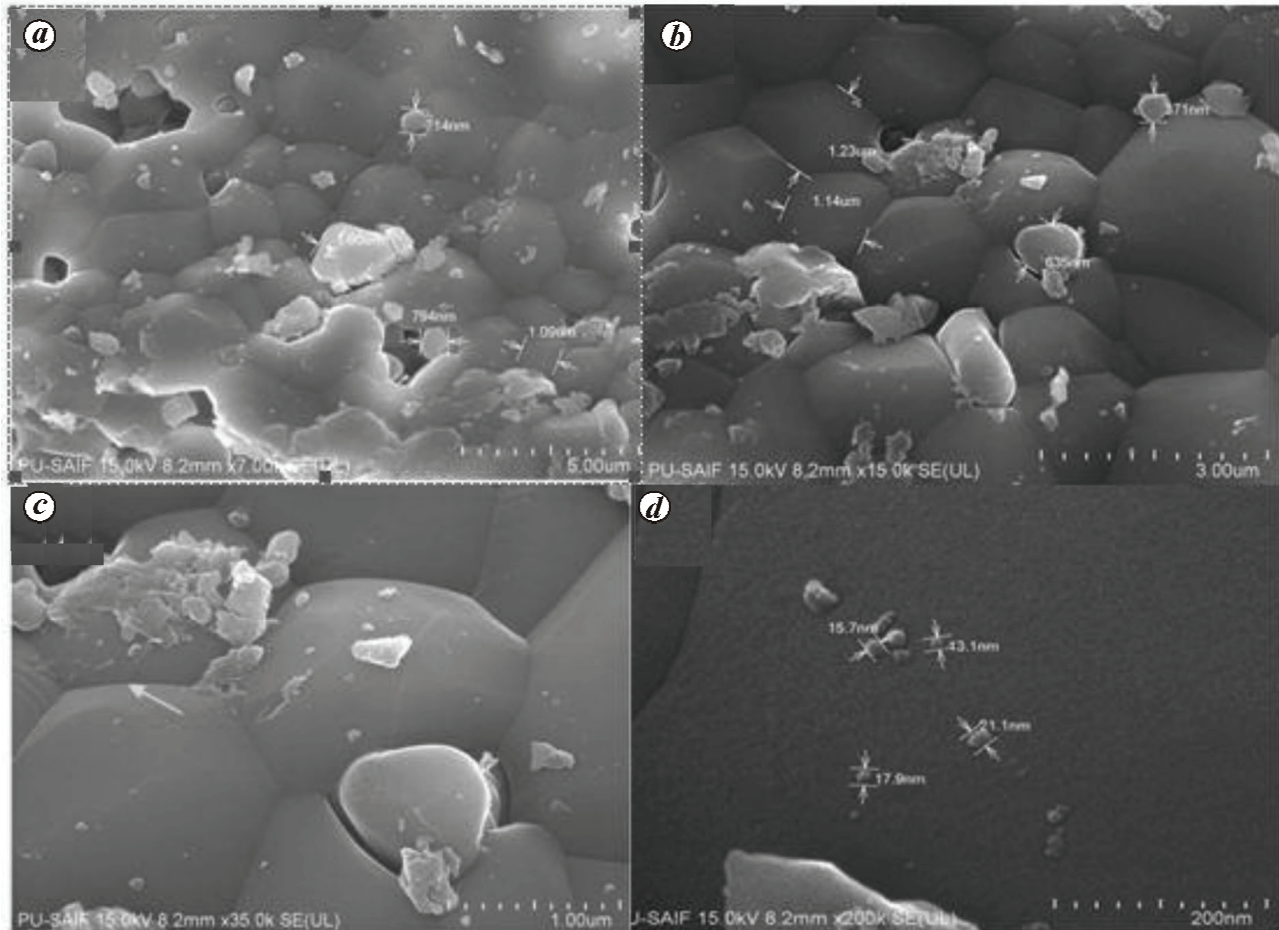


**Figure 1.** Field emission scanning electron photomicrographs of sintered ( $900^{\circ}\text{C}$ ) silver carp scale powder. **a, b**, Low magnification of compactly arranged hexagonal-shaped bioapatite particles of different sizes. **c, d**, Higher magnification reveals flat surfaces of these particles with scattered nanosized particles on the surface.

Hydroxyapatite is the main inorganic solid constituent of the hard tissue in bones. It has been extensively used as a filling material in the field of tissue engineering for bone tissue regeneration, especially as a scaffold material due to its well-known properties of excellent biocompatibility, bioactivity and osteoconductiveness<sup>3</sup>. Therefore, special attention is required for exploring new methods and then characterizing them for acquiring bioapatite of a particular structure and size from biogenic sources. Sintering is one such process in which particles of a powder are fused together by pressure and heated to a temperature below the melting point of the powder. The present study aims to gain a better understanding of the physico-chemical properties of fish bioapatite prepared by cryo-grinding technique to explore its desired application.

Silver carp (*Hypophthalmichthys molitrix*) was collected from the local fish market. The scales were gently removed, washed with distilled water and air-dried. They were then sintered in a quartz crucible at  $900^{\circ}\text{C}$  for 3 h in a muffle furnace, keeping the temperature below the

melting point of the major constituent of the bioapatite powder, which is  $900^{\circ}\text{C}$  for the scales of silver carp. Sintering is a heat treatment applied to a material for compacting in order to impart strength and integrity. The sintered fish scale flakes were manually ground to obtain fine crystals of bioapatite. The morphology, elemental analysis and particle size of the powder were examined by field emission scanning electron microscopy (FE-SEM) coupled with energy dispersive X-ray (EDS) (XFLASH 6130) for morphological analysis, dynamic light scattering (DLS) for hydrodynamic size analysis and Fourier transform infrared spectroscopy (FTIR) for chemical analysis.

The sintered powder was further subjected to cryogenic grinding in liquid nitrogen for 3 min which was repeated twice to allow better interaction of liquid nitrogen with the powder. The resultant powder was weighed and dissolved in ethanol (1 g in 10 ml ethanol). It was sonicated for 4 h and centrifuged at 2000 rpm for 5 min. The pellet was then discarded and the supernatant further centrifuged at

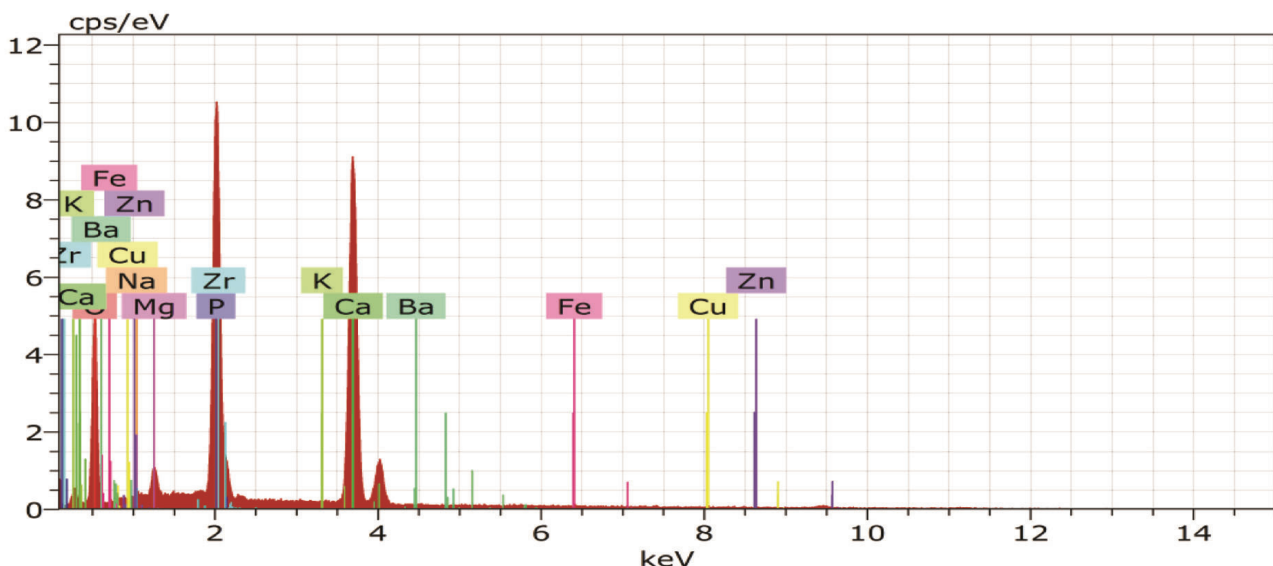


**Figure 2.** Energy dispersive X-ray spectroscopy graph of *Hypophthalmichthys molitrix* sintered scales showing the presence of elements and tetracalcium phosphate.

5000 rpm for 1 min. Then the suspension was again sonicated for 2 h and centrifuged for 5 min at 2000 rpm. The suspended particles were analysed to determine their size using DLS and transmission electron microscopy (TEM). FTIR was employed to examine if there were any structural changes.

Field emission scanning electron microscopy (FESEM) of the powder prepared after mechanical grinding of sintered fish scales revealed a heterogenous mixture of agglomerated hexagonal-shaped particles of irregular size range (micro- to nanosized) (Figure 1 *a* and *b*). Higher magnification of the same revealed that these particles had flat surfaces (Figure 1 *c* and *d*). Some stray nanosized particles were also observed scattered on the surface of these sub-micron-sized particles. Size of the particle is an important aspect of any implant material. It is considered that HAp nanoparticles can repair damage on the micro-metre-order, and such nanoparticles with smaller diameters promote faster recalcification<sup>4</sup>. The morphology of calcined, wet ball-milled and dried HAp powder also showed similar morphology comprising soft aggregated ultrafine particles<sup>3</sup>.

EDS is used for elemental analysis or chemical characterization of a material. The chemical composition of sintered (900°C) *H. molitrix* scale powder was analysed using EDS analyser. The results showed the presence of oxygen (40.12%), calcium (35.96%), phosphate (14.52%), zirconium (7.63%) and magnesium (1.16) in major quantity. Other elements present in lesser quantity were copper (0.20%), sodium (0.14%), barium (0.11%), zinc (0.07%), iron (0.03%) and potassium (0.03%) (Figure 2). From these results, the calcium/phosphate weight ratio for derived sintered scale powder was calculated as

1.97. The properties of calcium phosphates of biological interest depend strongly on their calcium/phosphate atomic ratios (Ca/P)<sup>5</sup>. From previous studies it is known that the calcium phosphate based powder having calcium/phosphate ratio around 2 (theoretical value) is tetracalcium phosphate,  $\text{Ca}_4(\text{PO}_4)_2$  (ref. 6). Hence it confirmed the presence of tetracalcium phosphate. This is a metastable compound and the only one with a calcium/phosphate ratio greater than HAp. It is an important ingredient in the self-setting calcium/phosphate bone cement<sup>7</sup>.

The core structure and morphology of cryoground powder were investigated by TEM. It was observed that the size of the particles was in the nanoscale with a mean particle size of  $120.5 \pm 47.85$  nm in diameter. The particles were found to be loosely aggregated (Figure 3 *a–c*). At higher magnification, the particles showed a flat and smooth surface (Figure 3 *d*). It was further revealed that individual particles were composed of small crystallites. Similar studies on the size and shape of nanoparticles obtained from biogenic hydroxyapatite have shown that important characteristics such as good bioactivity and flexible structure are preserved<sup>8</sup>. These nanoparticles are comparable to the size of biocrystal apatite<sup>9</sup> and exhibit rod-like shapes which probably are formed by fusion of fundamental blocks<sup>10</sup>.

FTIR was employed to characterize the different functional groups of sintered silver carp fish-scale powder. The FTIR spectra of tetracalcium phosphate and cryoground sintered scale powder were recorded in the range  $4000\text{--}400\text{ cm}^{-1}$ . Both spectra were almost similar and included a peak at  $1023\text{ cm}^{-1}$  that corresponded to the stretching of a phosphate group ( $\text{PO}_4^{3-}$ ). The broad band

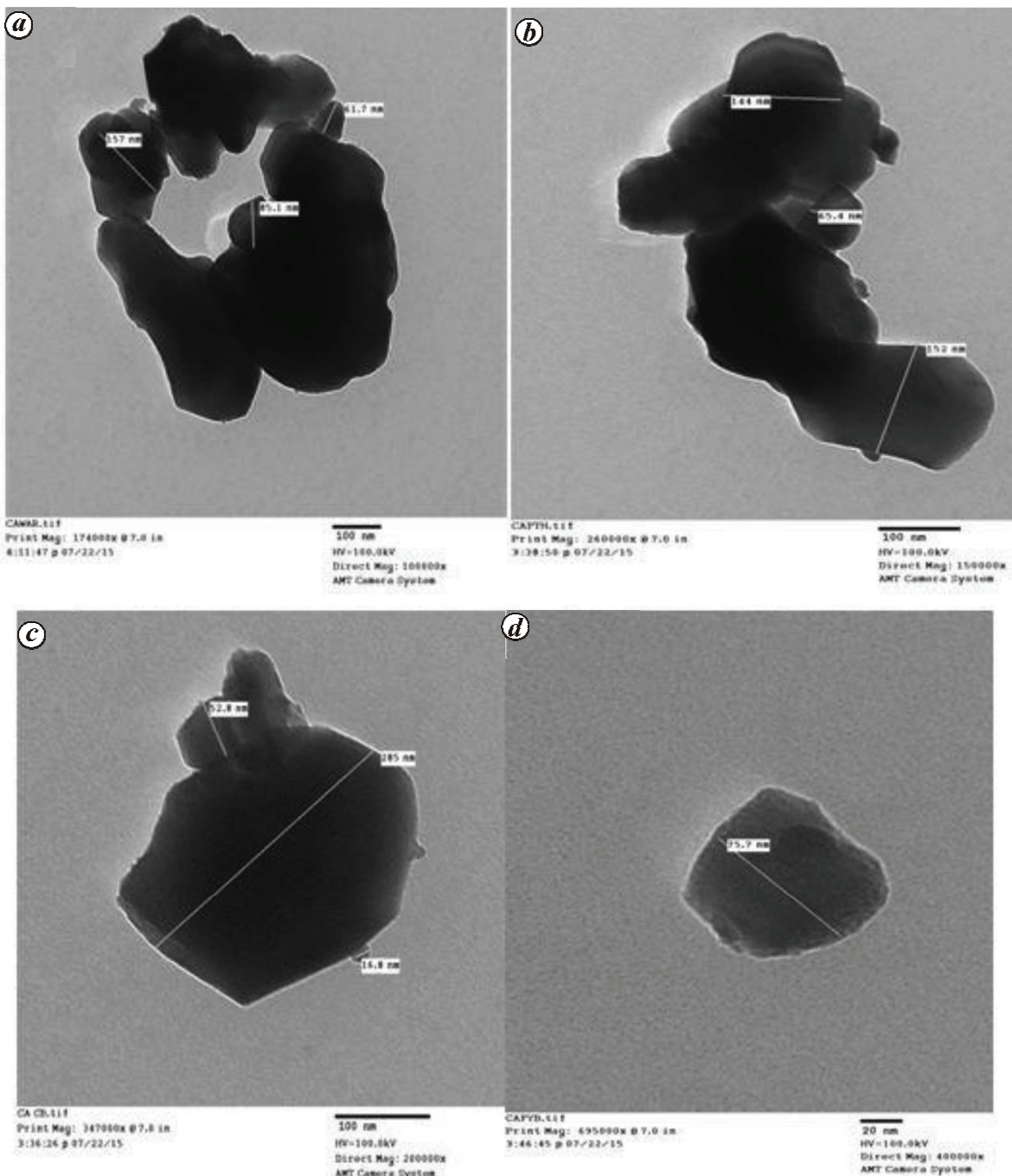


**Figure 3.** Transmission electron photomicrographs of silver carp scale bioapatite particles prepared by cryogenic grinding showing nanoscale particle (mean particle size  $120.5 \pm 47.85$  nm in diameter). **a–c**, Fish bioapatite particles are aggregated. **d**, Higher magnification of particles showing smooth surface with flat phase.

centred at about  $1000\text{--}1100\text{ cm}^{-1}$  was due to asymmetric stretching mode of vibration for  $\text{PO}_4$  group. The crystalline powder generated characteristic stretching modes of OH bands at about  $3422$  and  $496\text{ cm}^{-1}$ , which were noticed in the FTIR spectra of both tetracalcium phosphate and cryoground bioapatite. Sharp and strong bands assigned to the stretching mode of hydroxyl group at

around  $3572$  and  $632\text{ cm}^{-1}$  were observed in the spectra of synthetic hydroxyapatite<sup>11</sup>. The peaks obtained in the FTIR spectra of cryoground fish scale powder were more sharp and intense compared to the FTIR spectra of mechanically ground powder, which indicated that the cryoground bioapatite was more pure, as secondary phases such as calcium oxide were absent (Figure 4). It has been

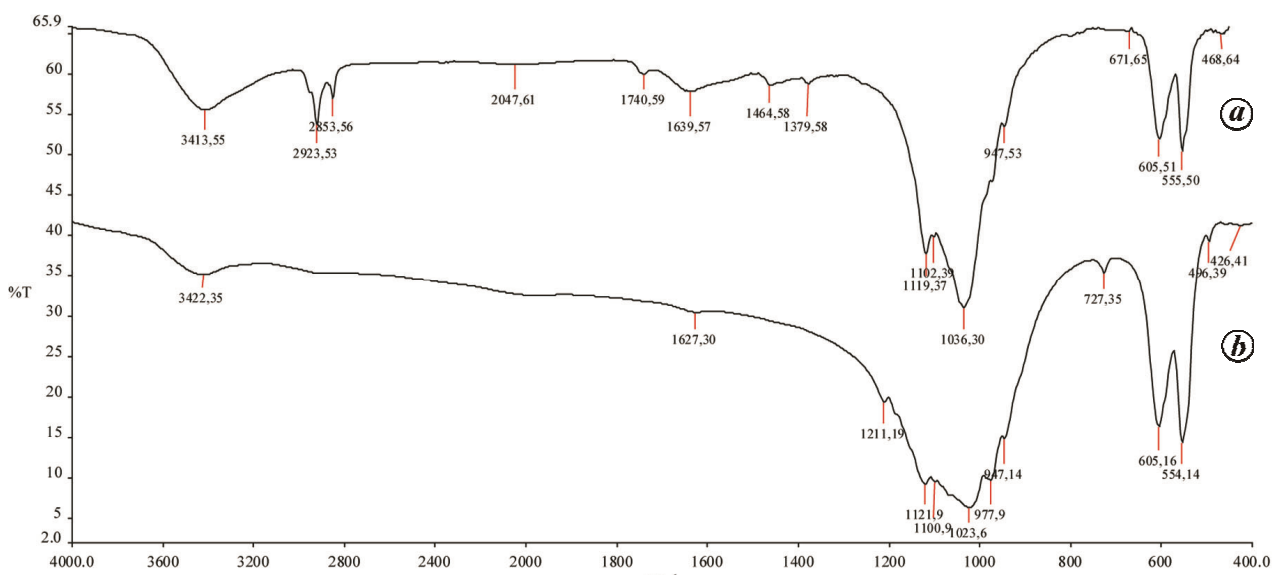


**Figure 4.** FTIR spectra of (a) cryogrinded *H. molitrix* scales and (b) sintered scale-derived tetracalcium phosphate.

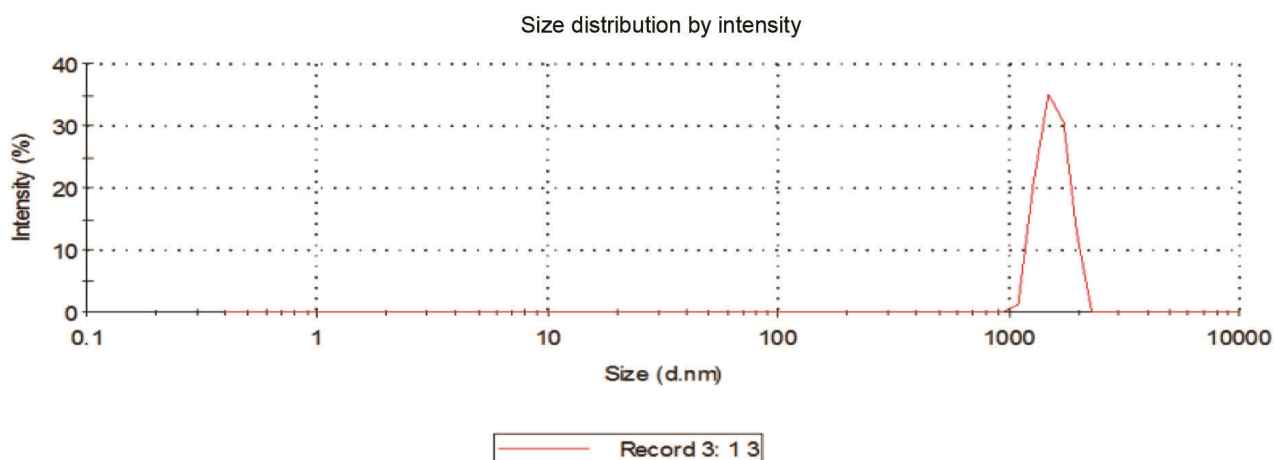


**Figure 5.** Particle size distribution of mechanically ground sintered silver carp scale powder.

reported that the fast cooling of sintered to tetracalcium phosphate (TTCP) by liquid nitrogen could avoid decomposition of the former and maintain its phase purity<sup>12</sup>. The particle size distribution of the obtained powders was also analysed using DLS. The particle size distribution of TTCP phosphate powder of sintered silver carp scale showed a broad size range of particles (1000–5000 nm); hence it is unsuitable for any application (Figure 5). Cryogrinding reduced the particle size of bioapatite to a mean value of 155.7 nm, thus providing better biogenic source (Figure 6). The average particle size (size of aggregates) of fish scale and synthetic body fluid synthesized HAp powders was 507 and 431 nm respectively, as observed using nanotrack analyser. These data indicate

comparable micromeric properties of HAp nanoparticles obtained from both sources for application in tissue engineering. These sub-micron-sized particles can be effectively used as biofillers<sup>13</sup>.

Thus, fish waste like scales can be utilized to produce useful nanosized BA<sub>p</sub> particles, which may have biomedical applications. Cryogrinding is an excellent processing technique through which sintered fish scales are converted into pure BA<sub>p</sub> with much smaller size (order of few nanometers). These nanosized particles which lie in narrow size range of about 120 nm have the potential for better bioresorbility and bioactivity in tissue engineering and replacements in comparison to large micron-sized particles. Hence cryogrinding is a novel processing step

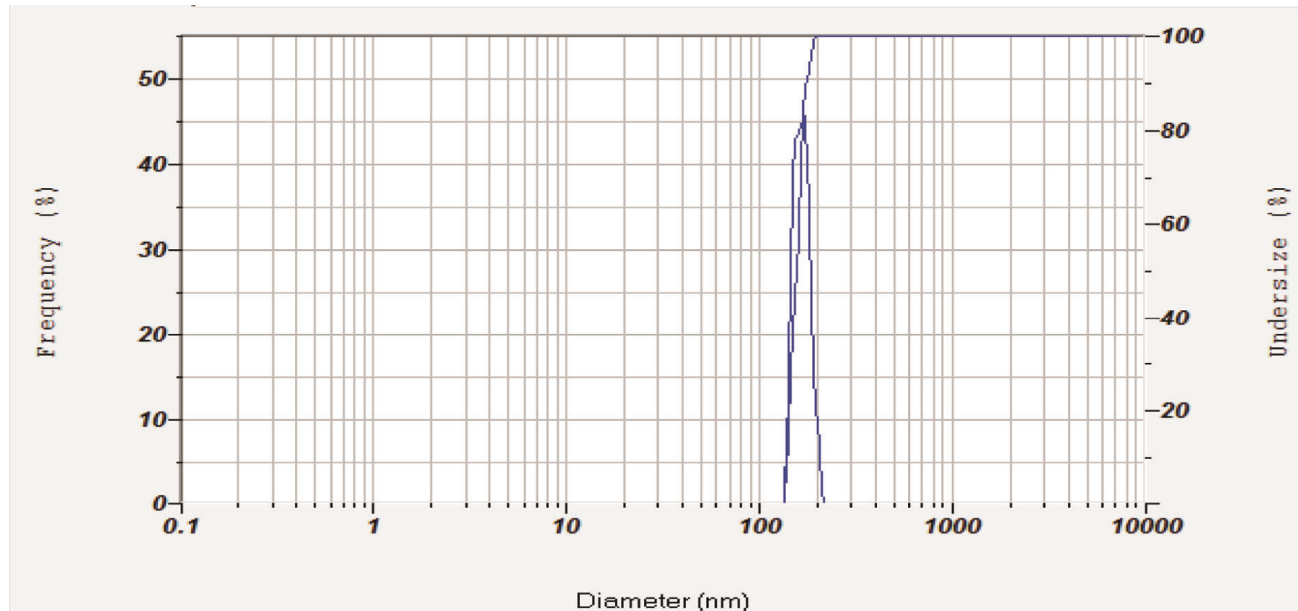


**Figure 6.** Particle size distribution of cryoground sintered silver carp scale powder.

which could be added to sintering of fish scales for better control over size and structure.

1. Supova, M. and Suchy, T., Bio-nanoceramics and bio-nano-composites. In *Handbook of Nanoceramic and Nanocomposite Coatings and Materials* (eds Makhlof, A. and Scharnweber, D.), Elsevier, Butterworth-Heinemann, Amsterdam, The Netherlands, 2015, pp. 29–58.
2. Scalera, F., Influence of the calcinations temperature on morphological and mechanical properties of highly porous hydroxyapatite scaffolds. *Ceram. Int.*, 2013, **39**, 4839–4846.
3. Mondal, S., Mondal, B., Dey, A. and Mukhopadhyay, S. S., Studies on processing and characterization of hydroxyapatite biomaterials from different biowastes. *J. Miner. Mater. Character. Eng.*, 2012, **11**, 55–67.
4. Iwamoto, T., Hieda, Y. and Kogai, Y., Effect of hydroxyapatite surface morphology on cell adhesion. *Mater. Sci. Eng. C*, 2016, **69**, 1263–1267.
5. Raynaud, S., Champion, E., Bernache-Assollant, D. and Laval, J. P., Determination of calcium/phosphorus atomic ratio of calcium phosphate apatites using X-ray diffractometry. *J. Am. Ceram. Soc.*, 2001, **84**, 359–366.
6. Habraken, W., Habibovic, P., Epple, M. and Bohner, M. Calcium phosphates in biomedical applications: materials for the future? *Mater. Today*, 2016, **19**, 69–87.
7. Moseke, C. and Gbureck, U., Tetracalcium phosphate: Synthesis, properties and biomedical applications. *Acta Biomater.*, 2010, **6**, 3815–3823.
8. Huang, J., Lin, Y. W., Fu, X. W., Best, S. M., Brooks, R. A., Rushton, N. and Bonfield, W., Development of nano-sized hydroxyapatite reinforced composites for tissue engineering scaffolds. *J. Mater. Sci.: Mater. Med.*, 2007, **18**, 2151–2157.
9. Posner, A. S., Crystal chemistry of bone mineral. *Physiol. Rev.*, 1969, **49**, 760–787.
10. Eppell, J. S., Tong, W., Katz, L. Z., Kuhn, L. and Glimcher, J. M., Shape and size of isolated bone mineralites measured using atomic force microscopy. *J. Orthop. Res.*, 2001, **19**, 1027–1034.

11. Varma, H. K. and Babu, S., Synthesis of calcium phosphate bioceramics by citrate gel pyrolysis method. *Ceram. Int.*, 2005, **31**, 109–114.
12. Kai, D., Fan, H., Li, D., Zhu, X. and Zhang, X., Preparation of tetracalcium phosphate and the effect on the properties of calcium phosphate cement. *Mater. Res. Forum*, 2009, **610–613**, 1356.
13. Panda, N. N., Pramanik, K. and Sukla, L. B., Extraction and characterization of biocompatible hydroxyapatite from freshwater fish scales for tissue engineering scaffold. *Bioprocess Biosyst. Eng.*, 2014, **37**, 433.

**ACKNOWLEDGEMENTS.** We thank UGC-CAS, DST-PURSE, TEQIP-II (Dr SSB UICET), UGC-SAP (Dr SSB UICET) for providing funds; Chairpersons, Department of Zoology and Chemical Engineering, Panjab University, Chandigarh for providing laboratory facilities, and FIST for instrumentation facilities to carry out this work.

Received 23 February 2017; revised accepted 24 May 2018

doi: 10.18520/cs/v115/i5/977-982